HAL open science

Quad-rotor MAV trajectory planning in wind fields

Jose Alfredo Guerrero, Juan Antonio Escareño, Yasmina Bestaoui

To cite this version:

Jose Alfredo Guerrero, Juan Antonio Escareño, Yasmina Bestaoui. Quad-rotor MAV trajectory planning in wind fields. IEEE International Conference on Robotics and Automation (ICRA 2013), May 2013, Karlsruhe, Germany. pp.778–783, 10.1109/ICRA.2013.6630661 . hal-00910993

HAL Id: hal-00910993

https://hal.science/hal-00910993v1

Submitted on 21 Jun 2022

HAL is a multi-disciplinary open access archive for the deposit and dissemination of scientific research documents, whether they are published or not. The documents may come from teaching and research institutions in France or abroad, or from public or private research centers.

L'archive ouverte pluridisciplinaire **HAL**, est destinée au dépôt et à la diffusion de documents scientifiques de niveau recherche, publiés ou non, émanant des établissements d'enseignement et de recherche français ou étrangers, des laboratoires publics ou privés.

Distributed under a Creative Commons Attribution - NonCommercial 4.0 International License

Quad-rotor MAV Trajectory Planning in Wind Fields

J.A. Guerrero, J.A. Escareno, Y. Bestaoui

Abstract— **This paper addresses the problem of time optimal path planning for a quadrotor helicopter evolving in a region of known winds. Usually, the flight control of quadrotors subject to wind disturbances challenge seeks to find the optimal control to keep track of a desired trajectory in a windy region. This approach has one major disadvantage: the quadrotor flight control has to compensate for trajectory deviations; therefore, the energy consumption becomes an issue. Most unmanned aerial vehicles (UAV) navigation techniques use waypoints to accomplish their missions. In the framework of a waypoint based navigation, a promising path planning strategy would be a time optimal approach in which the UAV would take advantage of wind to reach its next waypoint; therefore, saving time and energy (under constant forward velocity constraint). A model separation is used to simplify the control of the six-degrees-of-freedom (6DOF) dynamics of the quadrotor. Such approach allows to deal with quadrotor's 3D-motion through two subsystems: dynamic (altitude and MAV-relative forward velocity) and kinematic (nonholonomic navigation) subsystems. In terms of control, a hierarchical control scheme is used to stabilize dynamic and kinematic underactuated subsystems involved in the navigation task. The time optimal path planning is computed using a dynamic optimization method for continuous systems with some state variables specified at an unspecified terminal time. Results have been validated in simulation.**

I. Introduction

The applications of Miniature Air Vehicles (MAVs) have widely diversified during the last years. They comprise both military and civilian, though the latter has had a lower development rate. The application scenarios range from homeland security, pipeline surveillance, nuclear facilities monitoring, natural disaster damage assessment, etc. These real-world missions evolve in outdoors environments where the autonomous aerial vehicles are exposed to adverse atmospheric conditions; most of times, a windy environment. The majority of real-world MAV missions evolve in a waypoint navigation framework. An intuitive solution is to use a wind compensation approach which aims to compensate MAV trajectory for disturbances due to meteorological phenomena; therefore, energy consumption becomes an issue. For this reason, navigation methods that take advantage of wind velocity and direction are required to achieve the guidance objective between two any given waypoints; therefore, saving energy.

The literature in MAV guidance in regions of mild winds is vast and particularly focused on fixed-wing configurations and blimps. As in [1] where the authors use a linear quadratic regulator for optimal guidance of a fixed-wing MAV. The controller, evaluated at simulation level, aims to follow a straight-line and circular paths under different constant wind values. In [2] is experimentally implemented a path following controller using constant-velocity MAV under moderate wind conditions (20% to 50% of MAV airspeed). In [3] is presented a path planning and control algorithms meant to survey multiple-waypoints while considering heading and constrained rate heading. The path planning is treated as an optimization problem and assumes the knowledge of the constant wind component, while the sliding surface controller is aimed at dealing with small time varying wind components. A nonlinear controller is presented in [4] regarding to the following of a straight-line reference considering various constant lateral wind components (crosswind) up to 40% of the MAV speed.

Time optimal aircraft guidance in presence of winds has been discussed in [6] and [7]. [6] presents an aircraft routing algorithm to determine a minimal time path for an airplane using a Bolza problem approach. In [7], a neighboring optimal control approach has been adopted to obtain near-optimal trajectories using nominal solutions to the Zermelo problem. Both approaches consider the kinematic model of the aircraft, evolving in the 2D space, in the optimization problem. Optimal path planning between two waypoints considering the presence of obstacles and no-fly zones have been discussed in [5] and [9]. In[5] a trajectory planning is presented. This approach considers the use of core path graphs and optimal control in order to obtain an optimal trajectory between the origin and the destination while avoiding both obstacles and no-fly zones. The results were validated in simulation considering 2D and 3D cases. A lexicographic approach to optimal trajectory planning for the departure of aircrafts considering no-fly zones has been addressed in [9]. By using this approach, the optimization objectives can be ordered hierarchically. Recently, in [10] a trajectory planning for bridge inspection using harmonic potential functions has been presented. [11] presents an analysis of the time optimal trajectories of an airship. The time optimal problem is formulated as a generalization of the Zermelo's navigation problem. An analysis of the Lagrange multipliers and the set of solutions is presented.

This paper presents a hierarchical control architecture for time optimal quadrotor helicopter flying in a region of a-priori known winds. A simplified 3D model is used by splitting the 6DOF dynamics into two subsystems: a dynamic (forward velocity and altitude) subsystem and a kinematic (navigation) subsystem. Likewise, a hierarchical control scheme is used to stabilize underactuated dynamics

J. A. Guerrero (jguerrer@ieee.org) is with Irstea, TSCF Unit, Centre of Clermont- Ferrand, 24 avenue des Landais BP50085, Aubiere Cedex, France. J.A. Escareno is with Departement Automatique et Systemes Micro-Mecatroniques, FEMTO-ST Institute, UMR CNRS 6174, Besancon, France. Y. Bestaoui is with the IBISC laboratory, Université d'Evry Val d'Essonne.

and kinematics involved in the navigation control task. A nonlinear bounded controller is used to stabilize the angular error dynamics regarding to avoid singularities and actuators limits. A time optimal path planning is developed considering an evolution of the aerial robot in the 3D space. The resulting path is then used as the reference path to be followed by the nonlinear bounded controller. Simulations results shows the validity of the proposed approach.

This work is organized as follows: the dynamic model of the quadrotor is presented in section 2. The time-optimal path planning is presented in section 3. Section 4 presents the control strategy. Numerical simulations results are presented in Section 5. Conclusions and perspectives are finally given in Section 6.

II. Quadrotor Dynamic Model

A. Quadrotor Kynodynamic Model

In this section a two-rotational coupled model is presented to drive the aerial robot through the 3D space, with the aim of simplifying the navigation control task performed by the vehicle (Fig. 1).

- A regulated roll motion having small angular fluctuations is assumed.
- Pitch rotation $\mathcal{R}^{\theta}$ defines a dynamic subsystem containing altitude and MAV's relative motions.
- Yaw rotation $\mathcal{R}^{\psi}$ applied to velocity vector $\mathbf{V}_r$ yields a kinematic motion subsystem.

1) Dynamic subsystem (D-plane): This motion subsystem arises from the coordinate transformation $\mathcal{R}^{\theta}$, about e_2, applied to the main thrust vector $\mathbf{T}^b$, which leads to the well-known 3DOF longitudinal dynamics. Translational and rotational dynamics evolve within the plane resulting plane $e_x^{\theta} e_z^{\theta}$ called from now on D-plane. The advantage of this plane is that gravity might be included in the dynamic equations since the coordinates transformation from the inertial to the actual frame has no effect on gravity vector. The corresponding equations are given next

$$\begin{array}{l} (\Sigma_{D_t}): \\ (\Sigma_{D_r}): \end{array} \left\{ \begin{array}{rcl} m\dot{v}_r & = & -T\sin\theta \\ m\ddot{z} & = & -T\cos\theta + mg \\ I_y\ddot{\theta} & = & \tau_{\theta} \end{array} \right. \tag{1}$$

where v_r stands for the magnitude of the linear velocity relative to the quadrotor $\mathbf{V}_r$, T is the magnitude of $\mathbf{T}^b$, m is the mass of the vehicle which in the following is normalized to 1, τ_{θ} is the pitch control input.

2) Kinematic subsystem (K-plane): The transformation $\mathcal{R}^{\psi}$, about e_z^{ψ}, drives the dynamic plane according to heading motion. Therefore, $\mathbf{T}_x^{\theta}$ generates a planar translational motion along the inertial axes $e_x e_y$, called from now on K-plane (Kinematic plane). Provided that gravity is treated in the dynamic plane, then, it is more convenient to address vehicle's motion from a kinematic viewpoint, i.e. focusing on motion subsystem resulting from heading the relative velocity vector $\mathbf{V}_r$. The latter is expressed by the following

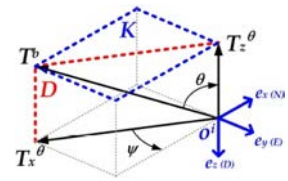

Fig. 1. D-K Planes

expressions

$$\begin{array}{l} (\Sigma_{K_t}): \\ (\Sigma_{K_r}): \end{array} \left\{ \begin{array}{rcl} \dot{x} & = & -v_r\cos\psi \\ \dot{y} & = & -v_r\sin\psi \\ I_z\ddot{\psi} & = & \tau_{\psi} \end{array} \right. \tag{2}$$

where τ_{ψ} is the yaw control input.

In the following section, the time optimal path planning for an aerial vehicle evolving in the 3D space is presented. It will be shown that the kinematic model of the quadrotor helicopter can be obtained from the general 3D kinematic model of an aerial vehicle.

III. Path Planning in Wind Fields

Lets consider the problem of a quadrotor helicopter flying in region of known winds available through meteorological forecasts or doppler radar measurements. The magnitude and the direction of the winds are known to be functions of position, i.e. $W_x = W_x(x,y,z)$, $W_y = W_y(x,y,z)$ and $W_z = W_z(x,y,z)$ where (x,y,z) are rectangular coordinates and (W_x, W_y, W_z) are the velocity components of the wind. The quadrotor velocity relative to the air mass is V, a constant. The goal is to find the minimum-time path between a pair of waypoints. The kinematic model of an aerial vehicle is given by

$$\begin{array}{rcl} \dot{x} & = & V\cos\chi\cos\gamma + W_x, \\ \dot{y} & = & V\sin\chi\cos\gamma + W_y, \\ \dot{z} & = & V\sin\gamma + W_z \end{array} \tag{3}$$

where χ is the heading angle of the aerial vehicle relative to the inertial frame, γ is the flight path angle. Notice that the kinematic model of the quadrotor in (2) previous section can be obtained from (3) using $\gamma = 0$. The heading angle χ is approximated by the yaw angle ψ and the velocity relative to the air mass V is approximated by the quadrotor forward velocity $-v_r$.

The time optimal trajectory generation can be formulated as follows:

$$\min \int_0^T dt \tag{4}$$

subject to

$$\begin{array}{rcl} \dot{x} & = & u_1(t) + W_x, \\ \dot{y} & = & u_2(t) + W_y, \\ \dot{z} & = & u_3(t) + W_z \end{array} \tag{5}$$

where $u_1(t) = V\cos\chi\cos\gamma$, $u_2(t) = V\sin\chi\cos\gamma$ and $u_3(t) = V\sin\gamma$; with the constraint $u_1^2(t) + u_2^2(t) + u_3^2(t) \leq V_{max}^2$. If the final waypoint is reachable at any time, then it is reachable in minimal time. However, if $W \gg V$, i.e. the

wind is too strong with respect the quadrotor velocity, there may be points that are not reachable at all.

The Hamiltonian of the system is

$$\begin{aligned} H =& \lambda_x(V\cos\chi\cos\gamma + W_x) + \lambda_y(V\sin\chi\cos\gamma + W_y) \\ &+ \lambda_z(V\sin\gamma + W_z) + 1. \end{aligned} \tag{6}$$

where λ_x, λ_y and λ_z are the Lagrange multipliers.

The Euler-Lagrange equations are

$$\dot{\lambda}_x = -\frac{\partial H}{\partial x} = -\lambda_x\frac{\partial W_x}{\partial x} - \lambda_y\frac{\partial W_y}{\partial x} - \lambda_z\frac{\partial W_z}{\partial x}, \tag{7}$$

$$\dot{\lambda}_y = -\frac{\partial H}{\partial y} = -\lambda_x\frac{\partial W_x}{\partial y} - \lambda_y\frac{\partial W_y}{\partial y} - \lambda_z\frac{\partial W_z}{\partial y}, \tag{8}$$

$$\dot{\lambda}_z = -\frac{\partial H}{\partial z} = -\lambda_x\frac{\partial W_x}{\partial z} - \lambda_y\frac{\partial W_y}{\partial z} - \lambda_z\frac{\partial W_z}{\partial z}, \tag{9}$$

$$0 = \frac{\partial H}{\partial \chi}, \tag{10}$$

$$0 = \frac{\partial H}{\partial \gamma}. \tag{11}$$

After some mathematical manipulation, it is easy to show that λ_x, λ_y and λ_z are given by

$$\lambda_x = \frac{-\cos\chi\cos\gamma}{\Lambda}, \tag{12}$$

$$\lambda_y = \frac{-\sin\chi\cos\gamma}{\Lambda}, \tag{13}$$

$$\lambda_z = \frac{-\sin\gamma}{\Lambda}. \tag{14}$$

where $\Lambda = V + W_x\cos\chi\cos\gamma + W_y\sin\chi\cos\gamma + W_z\sin\gamma$.

Introducing (12), (13), (14) into (7), (8), (9), we obtain

$$\begin{aligned} \dot{\lambda}_x =& \frac{\cos\chi\cos\gamma}{\Lambda}\frac{\partial W_x}{\partial x} + \frac{\sin\chi\cos\gamma}{\Lambda}\frac{\partial W_y}{\partial x} + \frac{\sin\gamma}{\Lambda}\frac{\partial W_z}{\partial x}, \\ \dot{\lambda}_y =& \frac{\cos\chi\cos\gamma}{\Lambda}\frac{\partial W_x}{\partial y} + \frac{\sin\chi\cos\gamma}{\Lambda}\frac{\partial W_y}{\partial y} + \frac{\sin\gamma}{\Lambda}\frac{\partial W_z}{\partial y}, \\ \dot{\lambda}_z =& \frac{\cos\chi\cos\gamma}{\Lambda}\frac{\partial W_x}{\partial z} + \frac{\sin\chi\cos\gamma}{\Lambda}\frac{\partial W_y}{\partial z} + \frac{\sin\gamma}{\Lambda}\frac{\partial W_z}{\partial z}. \end{aligned}$$

From previous equations it is easy to obtain an expression that describes the evolution of the heading angle and flight path angle,

$$\begin{aligned} \dot{\chi} =& \sin^2\chi\frac{\partial W_y}{\partial x} + \sin\chi\cos\chi\left(\frac{\partial W_x}{\partial x} - \frac{\partial W_y}{\partial y}\right) \\ &+ \sin\gamma\sec\gamma\left(\sin\chi\frac{\partial W_z}{\partial x} - \cos\chi\frac{\partial W_z}{\partial y}\right) - \cos^2\chi\frac{\partial W_x}{\partial y}, \end{aligned} \tag{15}$$

$$\begin{aligned} \dot{\gamma} =& \cos^2\chi\cos\gamma\sin\gamma\frac{\partial W_x}{\partial x} + \sin\chi\cos\gamma\sin\gamma\cos\chi\frac{\partial W_y}{\partial x} \\ &+ \sin^2\gamma\cos\chi\frac{\partial W_z}{\partial x} + \cos\chi\cos\gamma\sin\gamma\sin\chi\frac{\partial W_x}{\partial y} \\ &+ \sin^2\chi\cos\gamma\sin\gamma\frac{\partial W_y}{\partial y} + \sin^2\gamma\sin\chi\frac{\partial W_z}{\partial y} \\ &- \cos\chi\cos^2\gamma\frac{\partial W_x}{\partial z} + \sin\chi\cos^2\gamma\frac{\partial W_y}{\partial z} + \sin\gamma\cos\gamma\frac{\partial W_z}{\partial z}. \end{aligned} \tag{16}$$

A. Constant Wind

From (15) note that, if the W_x, W_y and W_z are constant, implies that $\chi = const.$, i.e., the minimum-time path are straight lines.

B. Linear Variation of Wind Velocity

Let V_w be the wind velocity, a constant. If $W_x(x,y) = \mp V_w y$ and $W_y(x,y) = 0$, it has been proved in [7] that

$$y = \frac{V}{V_w}\left(\frac{1}{\sin\chi} - \frac{1}{\sin\chi_f}\right), \tag{17}$$

$$\begin{aligned} x =& \frac{V}{2V_w}\left(\operatorname{asinh}(\tan\chi_f) - \operatorname{asinh}(\tan\chi) + \tan\chi\left(\frac{1}{\sin\chi} - \frac{1}{\sin\chi_f}\right)\right. \\ &\left. - \frac{1}{\cos\chi_f}\left(\tan\chi_f - \tan\chi\right)\right). \end{aligned} \tag{18}$$

where V_w is a positive constant, the wind velocity magnitude. The evolution of the heading angle χ and flight path angle γ is reduced to

$$\dot{\chi} = \pm V_w\cos^2(\chi). \tag{19}$$

and

$$\dot{\gamma} = \pm\, V_w\sin\gamma\sin\chi\cos\gamma\cos\chi. \tag{20}$$

The time to go is given by

$$T = \frac{1}{V_w}\left(\tan\chi_f - \tan\chi\right). \tag{21}$$

Notice that in the case of a quadrotor helicopter, the heading angle will be used as reference input for the kinematic control subsystem discussed in the following section. It is worth to mention that other vehicles may use both heading angle and flight path angle as reference inputs for the trajectory tracking control.

IV. Control Strategy

The navigation control design relays on three modules or subsystems: D-plane, K-plane and path planning subsystems. Within D-plane the controller aims to define the relative MAV velocity vector $\mathbf{V}_r$ and desired altitude, while in the K-plane whose controller aims to steer $\mathbf{V}_r$ so that the vehicle follows the desired path given by the path planning module. These subsystems are coupled via $\mathbf{V}_r$ generated by the dynamic subsystem and fed to the kinematic subsystem to perform the navigation task and ψ^d generated by the path planning module and provided to the kinematic subsystem as a reference input (Fig. 2).

A. Dynamic controller

At this level, our aim is to synthesize a control algorithm to achieve the desired references of drone-relative velocity and altitude, that is to say, errors $\bar{v}_q = v_r - v_r^d$ and $\bar{z} = z - z^d$ are rendered to zero. The desired forward velocity and altitude are defined as

$$v_r^d := a_r \tag{22}$$

$$z^d := a_z \tag{23}$$

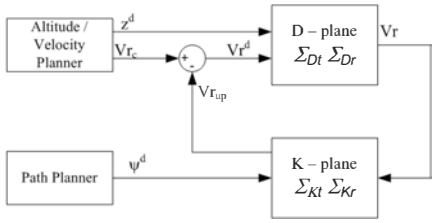

Fig. 2. Coupling between D- and K-planes

where a_r and a_z are positive constants. To stabilize the subsystem (1) we assign a linear stable behavior to translational dynamics Σ_{D_T} through polynomials $r_1(\bar{v}_r)$ and $r_2(\bar{z}, \dot{z})$ as presented in [12].

$$\begin{array}{rclcl} \dot{v}_r & = & -T\sin\theta & := & r_1(\bar{v}_r) \\ \ddot{z} & = & -T\cos\theta + g & := & r_2(\bar{z}, \dot{z}) \end{array} \tag{24}$$

Such stable behavior is achieved provided that desired values are achieved

$$T^d := \left[r_1^2 + (r_2 + g)\right]^{\frac{1}{2}} \tag{25}$$

$$\theta^d := \arctan 2\left(\frac{r_1}{r_2 + g}\right) \tag{26}$$

where, $r_1 = k_{p_r}\bar{v}_r$ and $r_2 = k_{p_z}\bar{z} + k_{v_z}\dot{z}$, with k_{p_r}, k_{p_z} and k_{v_z} being positive constants. Equations corresponding to desired thrust (25) and pitch (26) represent the components of the control vector in the dynamic plane.

Assumption **A1**. The present control design assumes that translation and rotational dynamics evolves in different scales of time, i.e. slow time-scale for translational and fast time-scale rotational motion.

The stabilization of (24) assumes $\theta = \theta^d$, which is valid provided the time-scale separation between translational and rotational dynamics. The latter implies the stabilization of the error dynamics,

$$\ddot{\tilde{\theta}} = \tau_\theta - \ddot{\theta}^d \tag{27}$$

Let us define the error as

$$\tilde{\theta} \triangleq \theta - \theta^d \tag{28}$$

The control design for the rotational inner-loop assumes the following:

- *Assumption* **A2**. Limited response of the torque actuators (rotors differential thrust) is assumed, i.e. $|\tau_\theta| \leq \tau_{\theta_{max}}$ with $\tau_{\theta_{max}} > 0$.
- *Assumption* **A3**. $\dot{\tilde{\theta}}$, is assumed bounded due to actuators saturation, i.e. $|\tilde{\theta}_2| \leq \delta$ with $\delta > 0$.
- *Assumption* **A4**. θ^d is a smooth time-varying function with its derivatives bounded.
- *Assumption* **A5**. Considering a non-aggressive translational trajectories the heading reference acceleration might be disregarded.

To design the control law for the inner-loop heading dynamics, we proceed similarly as in [13], where a backstepping-based controller is obtained considering a bounded velocity state (see **A2** and **A3**). Let us consider the Candidate Lyapunov Function (CLF) to obtain the controller that stabilizes the system (27)

$$\mathcal{W}_1 = \ln\cosh(\tilde{\theta}) \tag{29}$$

whose time-derivative is

$$\dot{\mathcal{W}}_1 = \dot{\tilde{\theta}}\tanh(\tilde{\theta}) \tag{30}$$

From the latter, it is clear that via $\dot{\tilde{\theta}}$ is possible to render $\mathcal{W}_1 < 0$ by using $\dot{\tilde{\theta}} = -\tanh(\tilde{\theta})$. Thus, the next step considers $\tilde{\theta}_2^d = -\tanh(\tilde{\theta})$ leading to the following error state

$$z = \dot{\tilde{\theta}} + \tanh(\tilde{\theta}) \tag{31}$$

where, for simplicity, we have considered a normalized value of m. The corresponding time-derivative is written

$$\dot{z} = \tau_\theta - \ddot{\tilde{\theta}}^d + \dot{\tilde{\theta}}\text{sech}^2(\tilde{\theta}) \tag{32}$$

Let us propose the overall CLF encompassing $\mathcal{W}_1$ as

$$\mathcal{W} = \ln\cosh(\tilde{\theta}) + \frac{1}{2}z^2 \tag{33}$$

whose the time-derivative is

$$\dot{\mathcal{W}} = \dot{\tilde{\theta}}\tanh(\tilde{\theta}) + z(\tau_\theta + \dot{\tilde{\theta}}\text{sech}^2(\tilde{\theta})) \tag{34}$$

now, using $\text{sech}^2(\tilde{\theta}) \leq 1$, (31) and (32) as well as the controller

$$\tau_\theta = -2z + \ddot{\tilde{\theta}}^d \tag{35}$$

yields

$$\dot{\mathcal{W}} = -\tanh^2(\tilde{\theta}) - z^2 \tag{36}$$

which is negative definite and guarantees that the trajectories of the state vector $(\tilde{\theta}, z)^T$ converge asymptotically to the origin.

B. Kinematic controller

We proceed to design the controller to head the quad-rotor velocity $v_r \in D$ in such a way that the angular error is rendered to zero, which means that the desired path has been achieved. Unlike classical kinematic models where the heading rate ω_p is interpreted as the actual control input, in the present case, however, the control input is the torque τ_ψ. Hence, the kinematic subsystem is rewritten as

$$\dot{x} = -v_r\cos\psi \tag{37}$$

$$\dot{y} = -v_r\sin\psi \tag{38}$$

$$\ddot{\psi} = \tau_\psi \tag{39}$$

The subsystem (38-39) is stabilized through a hierarchical control scheme (two-time scale), considering the path deviation kinematics as the slow-time scale (outer-loop) and the heading dynamics as the fast time-scale (inner-loop). Since the quad-rotor kinematics is driven via the angle ψ, which is not a control but a state variable of the heading dynamics. Then, the heading is controlled by τ_ψ to track the stabilizing

control of the quad-rotor kinematics, this introduces the following error variable

$$\bar{\psi} = \psi - \psi_d \tag{40}$$

with ψ_d given by the path planning subsystem discussed in section III. Notice that the kinematic model of the heading subsystem is given by

$$\dot{\psi}_d = \mp V_w \cos^2 \psi \tag{41}$$

The control of the heading error dynamics ($\ddot{\bar{\psi}}$) requires the time derivative, acceleration, of (41) to guarantee the trajectory following. The corresponding error dynamics is thus written as

$$\ddot{\tilde{\psi}} = \tau_\psi - \ddot{\psi}_d \tag{42}$$

The controller used to attain the path-following objective follows a similar structure of (35), i.e.

$$\tau_\psi = -k_{v_\psi} \tilde{\psi} - k_{p_\psi} \tanh \tilde{\psi} + \ddot{\psi}_d \tag{43}$$

As a result, it is guaranteed that the state vector $(\tilde{\psi}, \dot{\tilde{\psi}})$ converges asymptotically to the origin, using similar stability analysis used for $\tilde{\theta}$. The it is possible to guarantee that the flying robot reaches the desired path.

V. Simulation results

To illustrate the proposed solution, numerical simulations were performed to evaluate the quad-rotor flight performance while navigating through a region of winds. In the case, the initial velocity of the quadrotor is $v_r = 0.4$m./sec, the initial altitude is 0.9m., the linear varying wind velocity is 0.022m/s. The desired altitude was fixed to 1m. while the desired cruise velocity was set to 0.5m./sec. Extensive cases have been studied, however, due to space limitations, three trajectories departing from the same coordinates $(-4, 4)$ are discussed in this section. The final waypoints are $(40, 4)$, $(40, 0)$ and $(40, -4)$. Using the Zermelo-based approach the initial and final headings as well as the time to go from departure waypoint to each final waypoint is presented in table I. The corresponding trajectories are depicted in Figure 3.

TABLE I

Time to go, initial and final headings departing from $(-4, 4)$

Destination (m)	Time (sec)	χ_0 (deg)	χ_f (deg)
$(40, 4)$	90.5505	315.13	44.87
$(40, 0)$	84.8267	313.29	38.76
$(40, -4)$	80.5021	310.93	31.64

The dynamic controller uses v_r as desired the velocity reference for the outer-loop controller. The underactuated subsystem $\dot{v}_r$-$\ddot{\theta}$ is successfully controlled through a hierarchical control scheme. The quad-rotor altitude controller achieves a constant desired altitude of 1m. The corresponding results are shown on Figures 4-6.

Concerning the kinematics evolving within K-plane, the hierarchical controller regulating the path deviation kinematics via the heading dynamics presents a satisfactory performance. Figure 7 illustrates the kinematic controller.

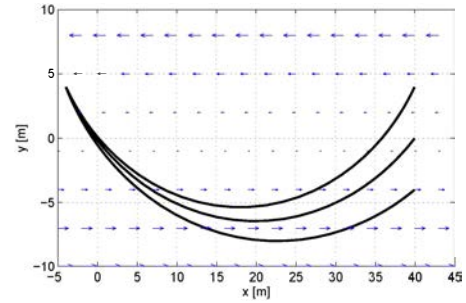

Fig. 3. Time-optimal trajectories considering linear varying wind.

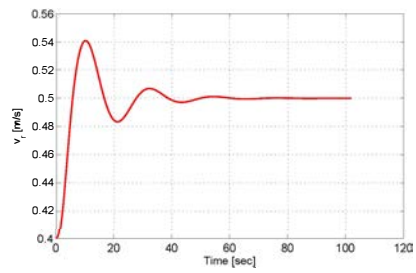

Fig. 4. Performance of the dynamic controller for v_r

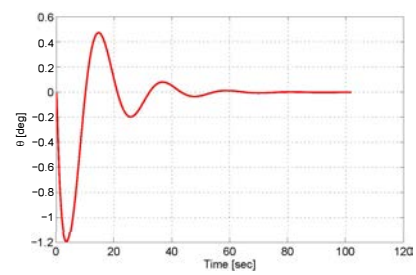

Fig. 5. Performance of the dynamic controller for θ

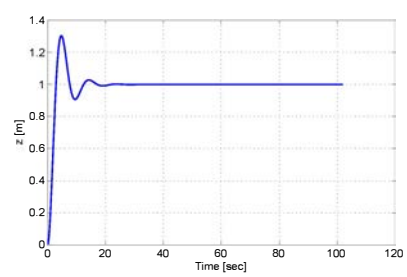

Fig. 6. Performance of the dynamic controller for altitude z

The tracking performance of the proposed control approach for quadrotor path planning and tracking in a region of winds is depicted in Figures 8-10.

A small deviation from the original time-optimal trajectory can be observed in Figures 8-10. This is assumed to be to the fact that the path planning module considers a constant velocity and the kinematic model considers a stable constant altitude. Notice that the initial velocity and altitude slightly differ from the desired velocity and altitude which may has

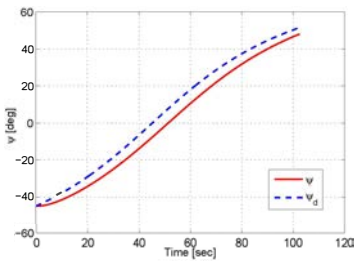

Fig. 7. Performance of the kinematic controller for heading.

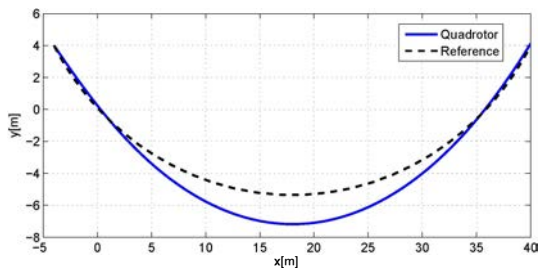

Fig. 8. Trajectory tracking in a region of winds with destination $(40, 4)$.

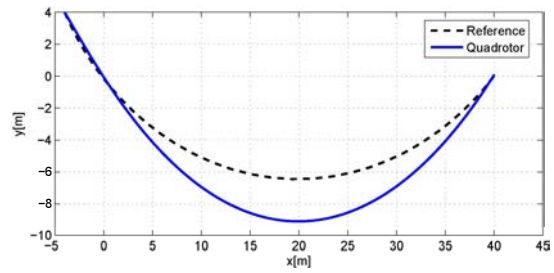

Fig. 9. Trajectory tracking in a region of winds with destination $(40, 0)$.

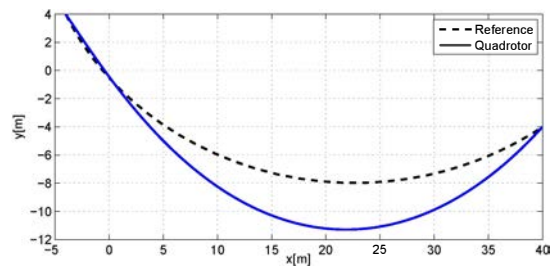

Fig. 10. Trajectory tracking in a region of winds with destination $(40, -4)$.

an impact on the tracking error.

VI. Concluding remarks and future works

The present paper proposes a model reduction regarding to simplifying the control task by partitioning the the complete dynamic model into a dynamic subsystem (D-plane) that focus to control forward velocity and altitude, and a kinematic subsystem (K-plane) that allows to treat the quad-rotor navigation problem as a nonholonomic-like path following. From this model simplification arises the possibility of applying a zermelo-based navigation scheme in the quad-rotor navigation flight with satisfactory results in simulations. The following objective is to validate the proposed approach by means of an experimental air platform to perform autonomous navigation in wind controlled situations. It is important that an outdoors application of the approach is considered by the authors, which implies an improvement in the kinematic subsystem control by designing robust algorithms that accounts the presence of external disturbances (e.g. wind gust).

VII. Acknowledgements

J.A. Guerrero thanks IBISC laboratory, Université d'Evry where he developed the time-optimal path planning for UAVs. He also thanks the LISTIC laboratory, Polytech Annecy for the support to complete this work.

References

[1] A. Ratnoo, P.B. Sujit and M. Kothari, "Adaptive Optimal Path Following for High Wind Flights", *IFAC world Congress*, Milano, 2011.

[2] D.R. Nelson, D. Blake, T. Barber, W. McLain, R.W. Beard, "Vector Field Path Following for Small Unmanned Air Vehicles", *IEEE American Control Conference*, Minneapolis, 2006.

[3] T.G. McGee, J.K. Hedrick, "Path Planning and Control for Multiple Point Surveillance by an Unmanned Aircraft in Wind", *IEEE American Control Conference*, Minneapolis, 2006

[4] A. Brezoescu, P. Castillo, R. Lozano, "Straight-line Path Following in Windy Conditions", *Conference on Unmanned Aerial Vehicle in Geomatics*, Zurich, Switzerland, 2011.

[5] M. Mattei and L. Blasi, "Smooth Flight Trajectory Planning in the Presence of No-Fly Zones and Obstacles", *in Journal of Guidance, Control and Dynamics*, Vol. 33, No. 2, 2010.

[6] S.J. Bijlsma, "Optimal Aircraft Routing in General Wind Fields", *in Journal of Guidance, Control, and Dynamics*, Vol. 32, No. 3, 2009.

[7] M.R. Jardin and A.E. Bryson Jr., "Neighboring Optimal Aircraft Guidance in Winds", *in Journal of Guidance, Control, and Dynamics*, Vol. 24, No. 4, pp.710-715, 2001.

[8] S.H. Pourtakdoust, M. Kiani and A. Hassanpour, "Optimal trajectory planning for flight through microburst wind shears", *in Aerospace Science and Technology*, Vol. , No., 2011.

[9] X. Prats, V. Puig, J. Quevedo and F.Nejjari, "Lexicographic Optimization for Optimal Departure Aircraft Trajectories", *in Aerospace Science and Technology*, Vol. 14, No., 2010.

[10] Y. Bestaoui, "Bridge Monitoring by a Lighter Than Air Robot", *in AIAA Aerospace Sciences Meeting including New Horizons Forum*, Orlando, Jan. 2011.

[11] Y. Bestaoui and E. Kahale, "Time optimal trajectories for an autonomous airship' *IEEE Workshop on Robot Motion Control (ROMOCO 2011)*, Bukowy Dworek, Poland, Juin 2011.

[12] R. Sepulchre, M. Jankovic and P. Kokotovic, Constructive Nonlinear Contro, Ed. Springer.

[13] K.B. Ngo, R. Mahony, J. Zhong-Ping, "Integrator backstepping design for motion systems with velocity constraint", *5th Asian Control Conference, 2004.*, Melbourne, Victoria, Australia, 2004.

[14] B. Herisse, F. Russotto, T. Hamel, R. Mahony, "Hovering flight and vertical landing control of a VTOL Unmanned Aerial Vehicle using Optical Flow", 2008 IEEE/RSJ International Conference on Intelligent Robots and Systems Acropolis Convention Center, Nice, France, Sept, 22-26, 2008